

Druggable glycolytic requirement for Hedgehog-dependent neuronal and medulloblastoma growth

Laura Di Magno^{1,2,3}, Daniela Manzi¹, Davide D'Amico¹, Sonia Coni^{1,3}, Alberto Macone⁴, Paola Infante^{1,2}, Lucia Di Marcotullio¹, Enrico De Smaele⁵, Elisabetta Ferretti⁵, Isabella Screpanti¹, Enzo Agostinelli^{3,4}, Alberto Gulino^{1,6,*}, and Gianluca Canettieri^{1,*}

¹Department of Molecular Medicine; Sapienza University of Rome; ²Center for Life Nanoscience@Sapienza; Italian Institute of Technology; Rome, Italy;

³Istituto Pasteur, Fondazione Cenci-Bolognetti; Sapienza University of Rome; Rome, Italy; ⁴Department of Biochemical Sciences; Sapienza University of Rome; Rome, Italy;

⁵Department of Experimental Medicine; Sapienza University of Rome; Rome, Italy; ⁶IRCCS Neuromed; Pozzilli, Italy

Keywords: cerebellum, DCA, glycolysis, Hedgehog, medulloblastoma, metabolism

Abbreviations: HH, Hedgehog; SHH, Sonic Hedgehog; MB, Medulloblastoma; HK2, Hexokinase 2; PKM2, Pyruvate Kinase M2; GCPs, granule cells progenitors; DCA, dichloroacetate; EGL, external granular layer; IGL, internal granular layer; Ptch1, Patched1; Smo, Smoothed; ATO, arsenic trioxide; ACC, Acetyl-CoA carboxylase; 2DG, 2-deoxy-D-glucose; ROS, reactive oxygen species; PARP, poly(ADP-ribose) polymerase; 3-BrPA, 3-Bromopyruvate; Sufu, suppressor of fused.

Aberrant activation of SHH pathway is a major cause of medulloblastoma (MB), the most frequent brain malignancy of the childhood. A few Hedgehog inhibitors, all antagonizing the membrane transducer Smo, have been approved or are under clinical trials for the treatment of human MB. However, the efficacy of these drugs is limited by the occurrence of novel mutations or by activation of downstream or non-canonical Hedgehog components. Thus, the identification of novel druggable downstream pathways represents a critical step to overcome this problem. In the present work we demonstrate that aerobic glycolysis is a valuable HH-dependent downstream target, since its inhibition significantly counteracts the HH-mediated growth of normal and tumor cells. Hedgehog activation induces transcription of hexokinase 2 (HK2) and pyruvate kinase M2 (PKM2), two key gatekeepers of glycolysis. The process is mediated by the canonical activation of the Gli transcription factors and causes a robust increase of extracellular lactate concentration. We show that inhibition of glycolysis at different levels blocks the Hedgehog-induced proliferation of granule cell progenitors (GCPs), the cells from which medulloblastoma arises. Remarkably, we demonstrate that this glycolytic transcriptional program is also upregulated in SHH-dependent tumors and that pharmacological targeting with the pyruvate kinase inhibitor dichloroacetate (DCA) efficiently represses MB growth *in vitro* and *in vivo*. Together, these data illustrate a previously uncharacterized pharmacological strategy to target Hedgehog dependent growth, which can be exploited for the treatment of medulloblastoma patients.

Introduction

Medulloblastoma (MB) is the most frequent brain malignancy of the childhood and is usually treated with a combination of surgery, chemotherapy and radiotherapy. The lethality of this tumor is about 30% and survivors often develop severe long-term neurological side effects, which have prompted effort to develop new therapeutic strategies.¹

MB originates from granule cell progenitors (GCPs),² a neuronal cell population that undergoes proliferation in the external granule layer (EGL) followed by migration in the internal granule layer (IGL) and differentiation into mature granules during cerebellar development.³ A leading cause of MB is the aberrant activation of the Sonic Hedgehog (SHH) pathway, a developmental signaling that regulates postnatal development of the cerebellum by promoting the mitotic expansion of GCPs in the EGL.⁴

Activation of the SHH pathway starts with the interaction of the ligand with the inhibitory receptor Patched1 (Ptch1), which causes the derepression of the transmembrane transducer Smoothed (Smo). Following ligand/receptor interaction, Smo migrates to the tip of the cilium, a microtubule based organelle, and triggers a series of intracellular events that terminates with the activation of the Gli transcription factors (Gli1, Gli2 and Gli3).⁵ The transcriptional targets regulated by SHH/Gli pathway have been in part elucidated and include genes involved in key cellular processes such as cell cycle, survival, migration and metabolism.⁶

Somatic or germline activating mutations of genes encoding SHH pathway components (i.e. Ptch1, Sufu, Smo, Gli2) have been found in MB patients belonging to the so-called SHH molecular subgroup.⁷ Furthermore, hyperactivation of SHH signaling, unrelated to genetic mutations, has been observed in MB and

*Correspondence to: Gianluca Canettieri; Email: gianluca.canettieri@uniroma1.it; Alberto Gulino; Email: alberto.gulino@uniroma1.it

Submitted: 07/02/2014; Revised: 08/04/2014; Accepted: 08/05/2014

<http://dx.doi.org/10.4161/15384101.2014.952973>

other tumors. For this reason, a substantial effort is being made to identify drugs that efficiently inhibit the SHH signaling.⁸

To date, most of the drugs found and tested in preclinical and clinical trials are Smo inhibitors. However, these compounds are not effective in case of mutations of components downstream of Smo or activation of non-canonical pathways, activating Gli. Additionally, despite the good initial response, patients treated with Smo inhibitors eventually develop resistance, due to the occurrence of novel mutations.⁸ For all these reasons, it is now widely believed that the development of drugs targeting downstream HH effectors would be a more appropriate strategy.

A few Gli inhibitors have been identified, such as GANT61 and arsenic trioxide (ATO) and they have shown a good inhibitory effect on HH-dependent transcription and MB growth *in vitro* and *in vivo*.^{9,10} However, none of these drugs have entered into clinical trials to date, mostly because their potential toxicity or lack of specificity is still a major concern.

A valuable approach, alternative to direct Gli inhibition, would be the identification of Gli-regulated events that are required for tumor growth and that could be targeted with drugs of known clinical efficacy.

In the present work we show that one of these druggable target is the metabolic reprogramming onto aerobic glycolysis, a process called Warburg effect that was recently described in Hedgehog-dependent cells and that is common to many highly proliferating and tumor cells.^{11,12} We illustrate that, through the canonical Gli-dependent pathway, Hedgehog governs a transcriptional program that shifts cell metabolism toward aerobic glycolysis. Importantly, we demonstrate that pharmacological inhibition of glycolysis efficiently counteracts tumor growth *in vitro* and *in vivo*, thus representing a promising avenue for the treatment of HH-dependent medulloblastoma.

Results

Hedgehog-induced GCPs proliferation requires glycolysis through the canonical pathway

Cell proliferation is an energy-demanding process that often relies on glucose and its metabolic reprogramming onto the glycolytic pathway to generate ATP and precursors.¹³ To study if HH-driven proliferation of GCPs selectively requires this glycolytic reprogramming, we measured BrdU incorporation in the presence of two different hexoses: glucose and galactose. Indeed, while glucose can be channeled into both aerobic glycolysis and oxidative phosphorylation cascades, galactose may only force cell metabolism toward mitochondrial oxidative phosphorylation.¹⁴ We used the concentration of 25 mM for both glucose and galactose to maintain the same osmotic pressure in the culture medium.¹⁵ In the presence of 25 mM glucose, GCPs proliferation was significantly induced by fifteen fold upon incubation of cells with SHH, compared to control, as evaluated by measuring the BrdU incorporation (Fig. 1A). In contrast, in the presence of the same concentration of galactose, SHH-induced GCPs proliferation was markedly reduced, thus indicating that proper HH-

induced proliferation of GCPs requires glucose, channeled toward the glycolytic pathway.

Previous studies in GCPs and medulloblastoma have shown a HH-dependent upregulation of hexokinase 2 (HK2) expression.^{6,11} In addition, the protein levels of PKM2, a key gatekeeper of the aerobic glycolytic pathway, were also found upregulated by SHH.¹⁶ To determine whether Hedgehog induces PKM2 at the mRNA level, we performed quantitative PCR. As shown in Figure 1B, both HK2 and PKM2 transcripts were significantly upregulated in GCPs, treated with SHH or the Smo agonist SAG. To study if this upregulation was Gli-dependent, we tested the effect of the Gli inhibitor arsenic trioxide (ATO).^{10,17} As shown in Figure 1C, ATO inhibited the SHH-induced increase of both mRNAs, demonstrating that the observed effect is mediated by the Gli transcription factors. Consistent with the upregulation of these glycolytic targets, treatment of GCPs with SAG induced a robust increase of the lactate released in the medium that was counteracted by ATO (Fig. 1D), thus indicating that the production of this metabolite is dependent on HH/Gli activation.

It was shown that, in metabolic tissues and fibroblasts, activation of Smo promotes a Warburg-like effect, through a rapid Gli-independent and AMPK-mediated activation of key glycolytic enzymes.¹⁸ Therefore, to further verify that lactate was produced by activation of Gli, we incubated GCPs with purmorphamine, a Smo agonist that selectively activates the canonical, Gli-dependent route.¹⁸ As shown in Figure 1E, purmorphamine increased HK2 and PKM2 mRNAs and the extracellular lactate content without affecting AMPK activity, as documented by the unchanged phosphorylation status of the AMPK substrate ACC. Conversely, ACC was efficiently phosphorylated in SAG-treated cells, confirming previous observations.¹⁸

Together, these data indicate that activation of the canonical Hedgehog signaling promotes glycolysis by upregulating PKM2 and HK2 mRNA levels via Gli.

We next wondered whether pharmacological inhibition of glycolysis counteracts GCPs proliferation. To this end, we measured BrdU incorporation of GCPs in the presence of dichloroacetate (DCA), a small molecule inhibitor of pyruvate dehydrogenase kinase, which promotes the entry of pyruvate into the TCA cycle and prevents the conversion of pyruvate to lactate.¹⁹ Incubation with DCA caused a dose-dependent inhibition of HH-induced GCPs proliferation (Fig. 2A). A similar effect was observed upon incubation of GCPs with two other inhibitors of glycolysis: 2-deoxyglucose (2DG), which inhibits the production of Glucose-6-phosphate, and 3-Bromopyruvate, a potent hexokinase II inhibitor (Fig. S1A and S1B), thus demonstrating that glycolysis is an essential and druggable metabolic requisite during HH-induced neuronal proliferation.

It was observed that DCA enhances apoptosis, by promoting mitochondrial glucose oxidation via the TCA cycle with consequent increased production of reactive oxygen species (ROS).¹⁹ Therefore we asked if, in addition to the observed inhibitory effect on cell proliferation, DCA treatment was also associated to increased apoptosis in Hedgehog-induced

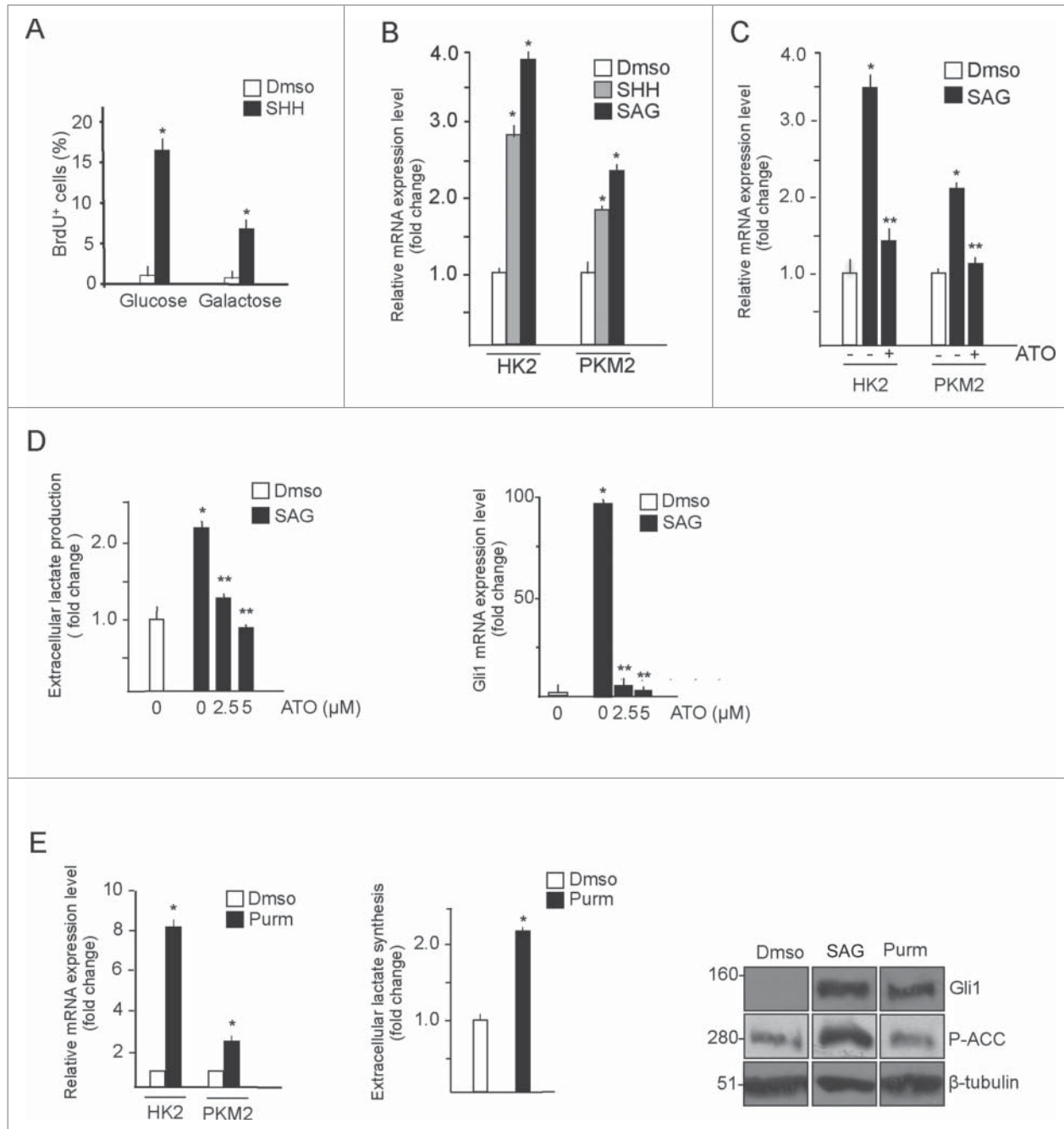


Figure 1. GCPs metabolic rewiring is sustained by canonical Hedgehog signaling. **(A)** GCPs proliferation requires glucose. BrdU assay in GCPs treated with SHH (3 $\mu\text{g}/\text{mL}$, 48 h) in the presence of glucose or D-galactose (25 mM, 48 hours). BrdU⁺ cells are expressed as a percentage of the total number of cells. Data represents the average \pm SD of 3 independent experiments. *SHH vs control, $P < 0.05$. **(B)** Quantitative real-time PCR from isolated GCPs demonstrates that Hedgehog agonists (SAG, 200 nM; SHH, 3 $\mu\text{g}/\text{mL}$, 48 hours) induce HK2 and PKM2 mRNA expression. *SHH and SAG vs control, $P < 0.05$. **(C)** Hedgehog-induced HK2 and PKM2 mRNA expression is mediated by Gli transcription factors. GCPs were treated with SAG (48 hours) and arsenic trioxide (ATO, 5 μM , 24 hours) and transcript levels were analyzed. *SAG vs control, $P < 0.05$; **ATO vs SAG, $P < 0.05$. **(D)** Left, dose-response effect of ATO in SAG-induced L-lactate production in GCPs. Values were normalized for cell number and expressed as fold change relative to vehicle-treated values. Right, quantitative real-time PCR analysis of Gli1 transcript levels to show efficacy of the treatments. *SAG vs control, $P < 0.05$; **ATO vs SAG, $P < 0.05$. **(E)** Purmorphamine (2 μM , 72 hours) increases HK2 and PKM2 transcription (left) and lactate synthesis (middle) in GCPs. Western blot analysis (right) shows that purmorphamine treatment has no effect on ACC phosphorylation whereas SAG does. *Purmorphamine vs control, $P < 0.01$; $n = 3$.

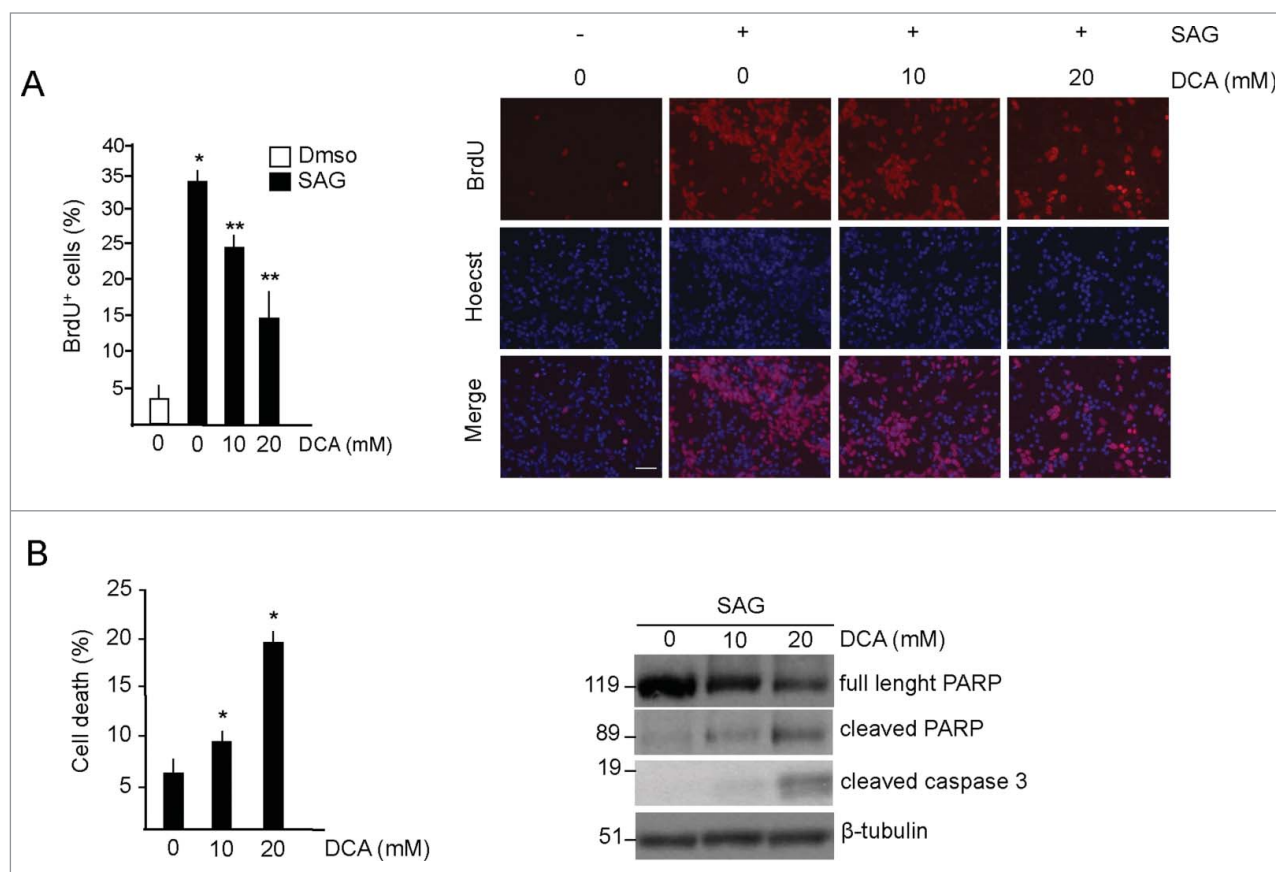


Figure 2. DCA decreases proliferation and induces apoptosis in GCPs. **(A)** Left, DCA decreases proliferation in GCPs. BrdU incorporation assay in cells treated with DMSO or with SAG (200 nM, 48 hours) and increasing amounts of DCA for 48 hours. BrdU was added for the last 24 hours. Right, representative images of BrdU staining. Scale bar = 50 μ m. *SAG vs control, $P < 0.05$; **DCA versus SAG, $P < 0.01$. **(B)** Left, DCA increases cell death in SAG-treated GCPs, as measured by the increase of the number of condensed and fragmented nuclei compared to control. Right, DCA increases active PARP and caspase 3. *DCA versus control, $P < 0.01$; $n = 4$.

GCPs. As shown in **Figure 2B**, DCA treatment increased the percentage of cell death and promoted apoptotic processes, as evaluated by the increased expression of caspase 3 and the induction of the 89 kD cleaved fragment of poly(ADP-ribose) polymerase (PARP).

Together, these data demonstrate that inhibition of glycolysis with DCA suppresses proliferation and induces apoptosis in SHH-treated GCPs.

Inhibition of glycolysis counteracts the growth of HH-dependent medulloblastoma

Having observed a druggable glycolytic requirement for HH induced GCPs proliferation, we next asked whether this mechanism could be exploited for treatment of HH-dependent medulloblastoma, a tumor that originates from GCPs when SHH signaling is aberrantly activated.²

Compared to normal cerebella, the content of HK2 and PKM2 mRNAs, as well as lactate, were strongly increased in medulloblastoma from Math1-Cre/Ptc^{fl/fl} mice, harboring conditional deletion of *Patched* (*Ptch*) in cerebellar Math1-expressing progenitor cells²⁰ (**Fig. 3A and B**).

Since the growth of these tumors is suppressed by the Smo inhibitor cyclopamine, we next tested the effect of this drug in the SHH induced metabolic reprogramming of MB cells. To this end, tumors were explanted, cultured and exposed to the Smo inhibitor cyclopamine, which caused a robust inhibition of cell proliferation, accompanied to a marked decrease of HK2 and PKM2 mRNA and of extracellular lactate concentration (**Fig 3C, D, E**). This indicates that the aberrantly activated HH-Gli signaling is responsible of the upregulated glycolytic transcriptional program in these tumors and suggests that the effect of cyclopamine involves the inhibition of metabolic reprogramming. To test if inhibition of glycolysis is efficient in counteracting the growth of SHH-MB tumors, we treated MB cells with DCA. The treatment led to a significant, dose-dependent reduction of cell proliferation, as evaluated by the analysis of BrdU incorporation (**Fig. 4A**). In addition, DCA promoted apoptosis of SHH-dependent MB cells as documented by the analysis of caspase 3 and cleaved PARP expression (**Fig. 4B**). As shown in **Fig. 4C**, extracellular lactate content decreased after DCA treatment in a dose-dependent manner. Therefore, these data indicate that

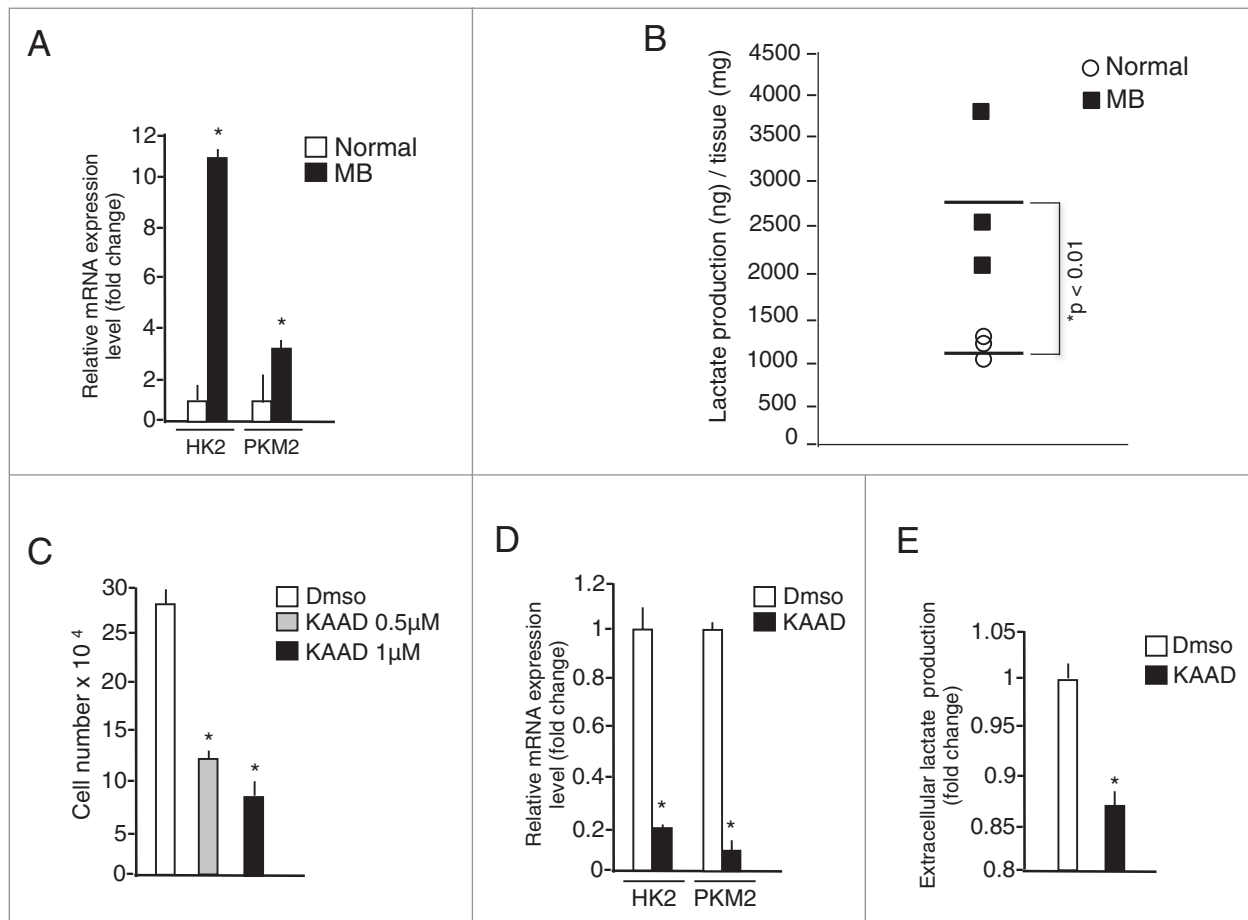


Figure 3. Medulloblastoma exhibits a glycolytic phenotype that can be reversed by cycloamine. **(A)** Quantitative real-time PCR analysis of HK2 and PKM2 mRNA expression in medulloblastoma from Math1-Cre/Ptc^{fl/fl} mice (MB) compared to normal adult mice cerebella (Normal). *MB versus Normal, $P < 0.05$; $n = 4$. **(B)** Local L-lactate concentration in medulloblastoma from Math1-Cre/Ptc^{fl/fl} mice compared to normal cerebella. Values are expressed as ng of lactate/mg of tissue. *MB versus Normal, $P < 0.05$. **(C, D)** MB neurospheres were incubated with 0.5 or 1 μ M cycloamine-KAAD for 48 hours and cell number was measured at the end of the treatment **(C)**. HK2 and PKM2 mRNA levels were assessed in 1 μ M Cycloamine-KAAD treated cells **(D)**. * $P < 0.01$ $n = 4$. **(E)** Cycloamine-KAAD treatment (1 μ M, 48 hours) decreases extracellular L-lactate levels in medulloblastoma cells cultures. Values were normalized for cell number and expressed as fold change relative to vehicle-treated values *Cycloamine-KAAD versus control, $P < 0.05$, $n = 3$.

glycolysis has the double effect of promoting growth and preventing apoptosis also in these cancer cells.

To analyze the effect of DCA in a preclinical setting, we allografted HH-dependent MB cells from Math1-Cre/Ptc^{fl/fl} mice into nude mice and administered 1.4 g/l DCA (corresponding to a calculated 100 mg/Kg/die, used in patients) in the drinking water, monitoring the tumor volume every other day. Compared to controls, tumors treated with DCA showed a significantly reduced growth rate (Fig. 5A), with an average tumor volume that was 3 times smaller than control at the end of the treatment (Fig. 5B) and this reduction was associated to a significant decrease of lactate content in tumors from DCA treated mice (Fig. 5C).

In keeping with the *in vitro* data, we observed a reduction of proliferating cells in tumor sections from DCA-treated mice, as evaluated by immunohistochemical analysis of Ki67 antigen. Additionally, tumors from DCA-treated mice showed increased caspase 3 staining, thus demonstrating that the same cascade of events observed in cell cultures also occurs *in vivo* (Fig. 5D).

Collectively, these data demonstrate that, by disrupting the glycolytic reprogramming, treatment with DCA has a powerful inhibitory effect on SHH-dependent tumor growth both *in vitro* and *in vivo*.

Discussion

The present work unmasks the high vulnerability of proliferating SHH-stimulated cerebellar progenitors and their tumor counterparts to pharmacological inhibition of aerobic glycolysis.

A work by Gershon and colleagues¹¹ showed that, by upregulating hexokinase 2 mRNA levels, HH signaling promotes metabolic rewiring toward aerobic glycolysis. This process, confirmed by our data, was shown to be required for proper GCPs and SHH MB proliferation and conditional deletion of HK2 gene in mice was able to attenuate medulloblastoma aggressiveness¹¹. In this work we have extended that observation and found that

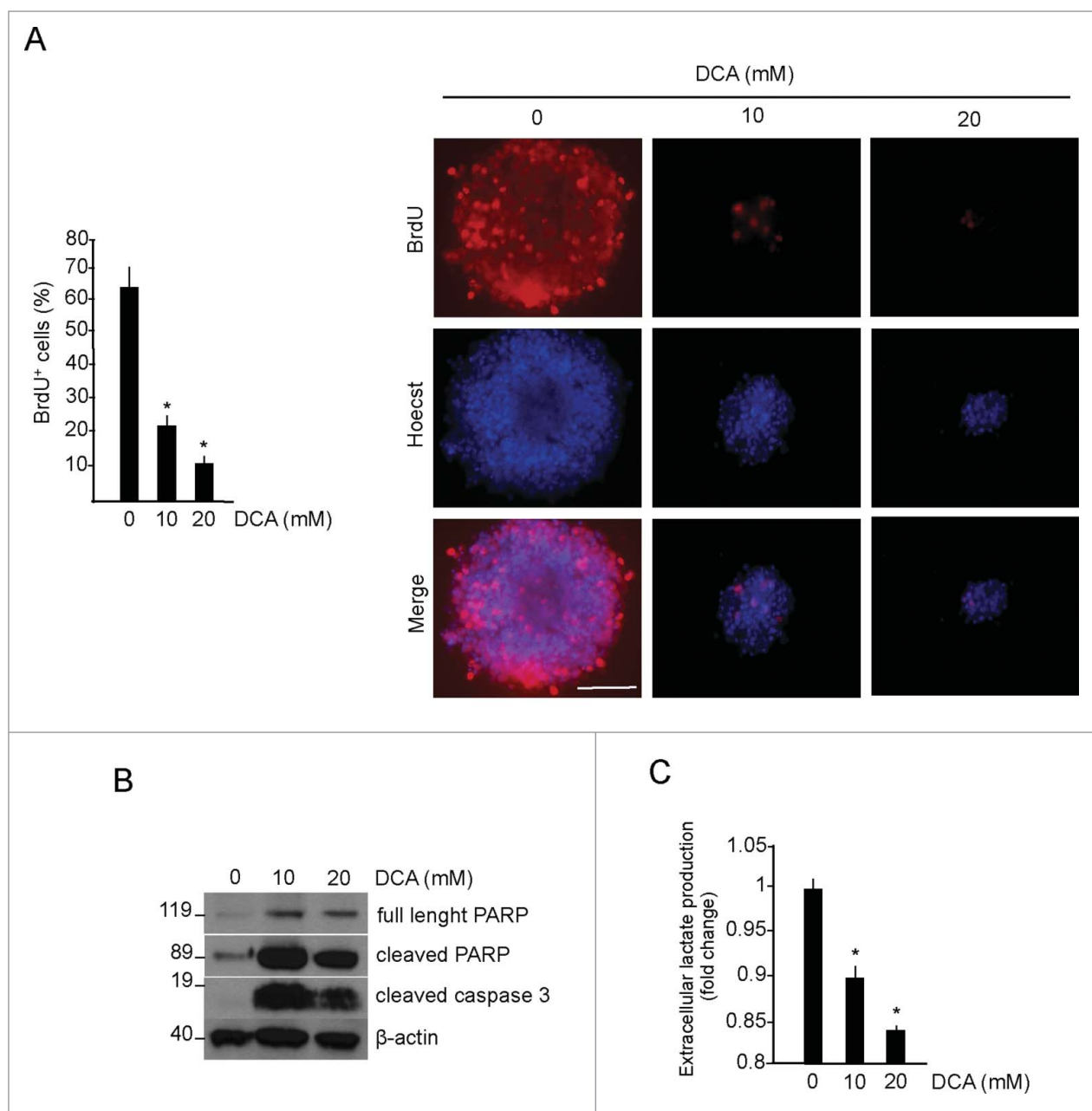


Figure 4. Glycolytic phenotype promotes proliferation and survival in medulloblastoma neurospheres. **(A)** DCA treatment (48 hours) of medulloblastoma neurospheres proliferation, measured by BrdU incorporation (red). Cells were counterstained by nuclear fluorescent stain Hoechst33342 (blue). Scale bar = 100 μ m. *DCA versus control, $P < 0.01$; $n = 4$ **(B)** Apoptotic markers (PARP and Caspase 3 activation) and β -actin levels (as loading control) were detected by Western blotting, $n = 4$. **(C)** L-lactate levels in MB neurospheres, treated as above. Values are expressed as fold change, relative to untreated cells. * $P < 0.01$; $n = 4$.

PKM2 mRNA levels are also upregulated by the Hedgehog pathway, thus contributing to the glycolytic reprogramming observed in GCPs and tumors.

The Warburg effect has been mainly explained as a mechanism used by the highly proliferating cells for a double purpose: i) to generate intermediates required to synthesize the macromolecules needed to build up the so-called biomass and ii) to prevent apoptosis due to the massive production of ROS generated by an upregulated TCA cycle.²¹

According to this view, we have observed that inhibition of glycolysis with DCA promotes a dual effect of inhibition of cell proliferation and induction of apoptosis.

In a previous work it was demonstrated that Smo activation in non-neuronal cells (adipocytes, muscle cells and fibroblasts) promotes a metabolic shift to the aerobic glycolysis, by activating a non-canonical, fast-acting route, involving Ca^{++} entry, activation of CamKK4 and AMPK-dependent phosphorylation of key glycolytic enzymes.¹⁸ Interestingly, the available Smo modulating

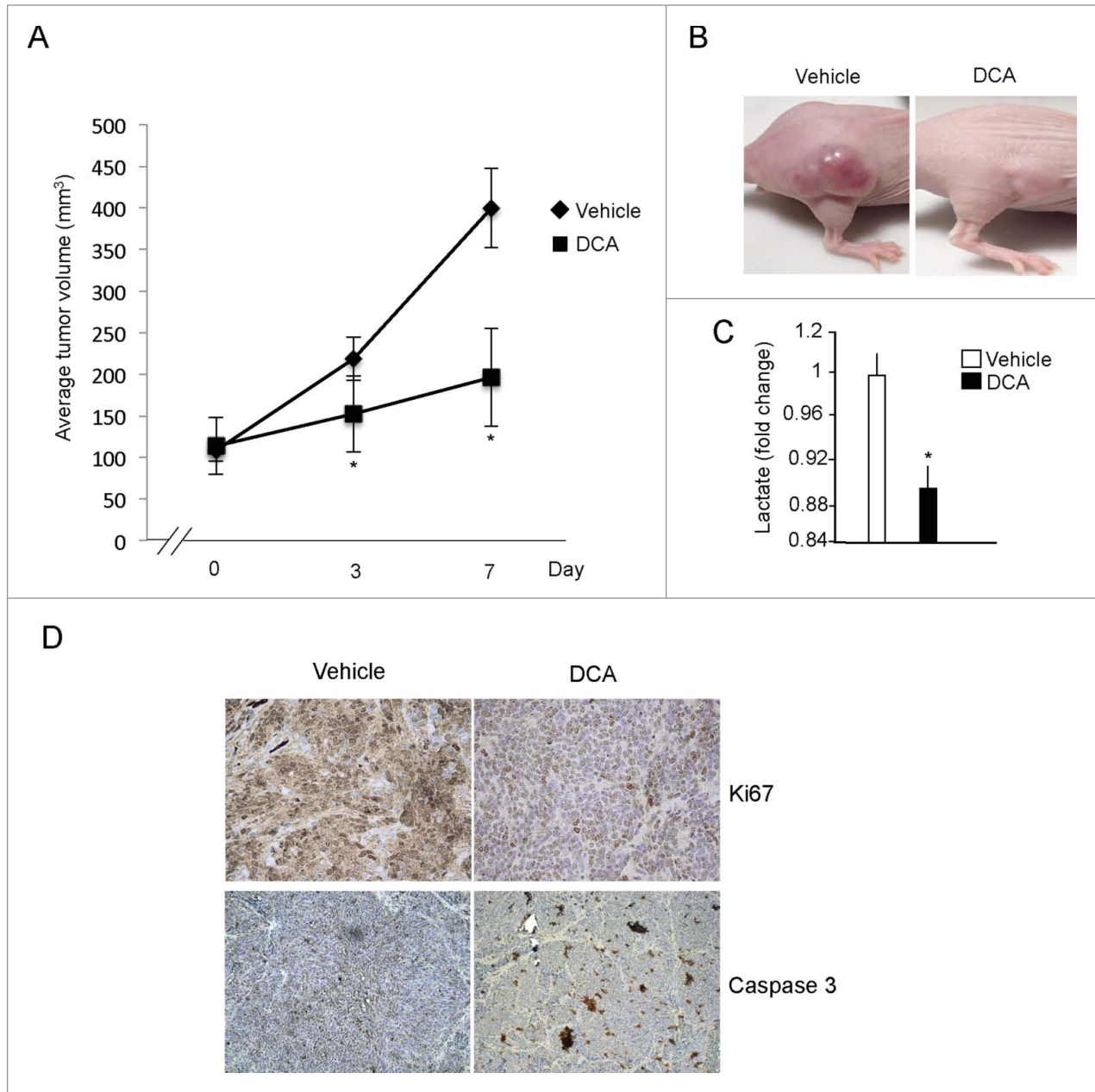


Figure 5. DCA decreases tumor size in medulloblastoma allograft models. **(A)** MB neurospheres were injected into the flanks of athymic mice and DCA (1.4 g/l) was administered in the drinking water. Measures were performed when tumors reached a measurable volume (day 0). **(B)** Representative images of tumors at the end of the treatment. Tumor size was measured by calipers *in vivo* and after euthanasia. *DCA versus vehicle, $P < 0.05$. **(C)** Local L-lactate concentration in tumors from vehicle-treated and DCA-treated groups. Values were normalized for tissue weight (mg) and expressed as fold change relative to control. Data represents the average \pm SD of 3 independent experiments. *DCA versus vehicle, $P < 0.05$ $n = 3$. **(D)** Immunohistochemistry of Ki67 and Caspase 3 expression in tumor sections from vehicle and DCA-treated mice.

compounds appear to exert distinct functions on the canonical vs non canonical Smo-AMPK axis. For instance, SAG seems to be able to activate both branches, while cyclopamine and purmorphamine appear to act as selective partial agonists on the non-canonical and canonical route, respectively. The ability of the canonical activator purmorphamine to significantly promote glycolysis and the strong inhibitory effect of the Gli inhibitor ATO on extracellular lactate concentration clearly indicate that a

major fraction of this metabolite in SHH-treated GCPs comes from Gli dependent mechanism.

A very relevant finding of this work is the effect of the glycolytic inhibitor DCA on SHH-dependent tumor growth.

We demonstrate here that a preclinical pharmacological approach targeting the same metabolic pathway can significantly limit the *in vivo* growth of SHH-dependent medulloblastoma. This observation is relevant since resistance to Smo antagonists is

a major burden in the treatment of medulloblastoma of the SHH subgroup and, despite the extensive investigation, clinically approved inhibitors of HH-regulated downstream effectors are still unavailable. Here we demonstrate that one of the effects of cyclopamine in these tumors is the inhibition of the Gli-mediated glycolytic program and lactate production, a process that is required for tumor growth *in vitro* and *in vivo*. Importantly, pharmacological inhibition of glycolysis suppresses SHH dependent tumor growth, therefore demonstrating that targeting this Gli-regulated process could be a valuable strategy to overcome the problem of resistance observed after treatment with Smo antagonists. However, since we used heterotopic flank allograft, further studies with orthotopic implantation of tumor cells will be required to properly evaluate the pharmacokinetics, drug distribution and long-term tumor response to this drug.

DCA is a small molecule that has a good safety profile and minimal side effects. It has been long used for the treatment of lactic acidosis linked to inherited mitochondrial diseases and in recent years has shown a significant antitumor activity in xenograft models of many forms of cancers.^{19,22-26} As for brain tumors, DCA has been tested in a clinical trial of glioblastoma multiforme (GBM)²⁷ and is still under evaluation (<http://clinicaltrials.gov/show/nct01111097>). Thus, this small molecule appears to be a good candidate for clinical trials in MB patients of the SHH subgroup. Further preclinical and clinical studies with this DCA, alone or in combination with other drugs, are required to clarify these critical aspects.

Materials and Methods

Reagents

D-Galactose, 2-deoxy-D-glucose, 3-BrPA, sodium dichloroacetate, arsenic trioxide were purchased from Sigma-Aldrich. 3-BrPA was prepared by dissolving the powder in PBS and adjusted to pH 7.0 with NaOH. Hedgehog agonists SAG (200 nM, Enzo Life Sciences), rmShh-N (3 µg/mL, R&D systems), Purmorphamine (2 µM, Millipore) were added to serum free medium. Cyclopamine-KAAD was purchased from Millipore.

Antibodies for immunostaining were obtained from commercial sources: GLI1, phospho-ACC, PARP, Caspase 3 were from Cell Signaling Technology, tubulin and actin were from Santa Cruz Biotechnologies.

Neurobasal medium, Neurobasal-A medium, Neurobasal-A medium without D-glucose, B27 supplement, B27 supplement minus vitamin A, HBSS were purchased from Life Technologies.

Cerebellar granules progenitors (GCPs) isolation and culture

Cultures of GCPs were carried out as described.²⁸ Cerebella were isolated from P7 mice, dissociated, plated onto poly-L-lysine-coated coverslips and allowed to adhere in Neurobasal medium, B27 supplement and 5% FBS. After 3 hours, medium was replaced with serum-free medium and cells treated with SAG. For 2-DG experiments, 2-DG was added to serum-free medium at the final concentration of 25 mM. For galactose experiments, media was replaced with Neurobasal A without

glucose and B27 supplement, and galactose was added at the final concentration of 25 mM, as previously reported.¹⁵

GCPs proliferation assays

3.5×10^5 GCPs were seeded in Neurobasal medium with 5% FBS onto poly-L-lysine-coated coverslips and allowed to adhere. After 3 hours, medium was replaced with serum free medium and cells were treated as indicated. BrdU was added to medium for the last 24 hours of treatment. GCPs were fixed with paraformaldehyde (4%) and immunostained with BrdU-labeling assay Kit (Roche). Stained cells were counted.

Medulloblastoma culture

MB cultures were derived from spontaneous, intracranial MB from Math1-Cre/Ptc^{fl/fl} mice. Tumors were removed, placed in HBSS and mechanically disrupted. The cellular suspension was digested with DNaseI (40 µL/mL, Sigma-Aldrich) for 30 minutes, mixing every 10 minutes. Cells were centrifuged at 1000 rpm for 5 minutes and the pellet suspended and cultured in Neurobasal Media-A with B27 supplement minus vitamin A, as previously described.²⁹

Medulloblastoma proliferation assay

Equal number of single cell suspension from freshly isolated MB was seeded and treated with the specific drugs for the indicated time. The resulting MB neurospheres were dissociated, mixed 1:1 with 0.4% Trypan blue dye and counted. For BrdU experiments, cells were treated with BrdU for 24 hours. MB neurospheres were then transferred onto poly-L-lysine-coated coverslips and allowed to adhere. The spheres were fixed and immunostained with BrdU-labeling assay Kit (Roche). Stained cells were counted.

Medulloblastoma allograft model

Freshly isolated MBs from Math1-Cre/Ptc^{fl/fl} mice were disaggregated and injected into athymic nude mice (Charles River Laboratories). 2×10^6 cells were suspended in PBS and mixed 1:1 with Matrigel (BD Pharmingen), and injected subcutaneously into the left and right flanks of ten mice (vehicle = 5, DCA = 5). DCA was added into sterile drinking water to reach the final concentration of 1.4 g/l, corresponding to the dosage used for clinical applications (100 mg/Kg/day). Tumor volumes were measured with a caliper, starting when the masses reached 100 mm³ volume, using the following formula: $V = (L \times W^2)/2$. Study events were recorded and analyzed using GraphPad Prism software (v5.0a).

The local Ethics committee approved all the reported procedures involving mice.

Quantitative real-time PCR

RNA extraction and quantitative real-time PCR were performed as described.^{30,31}

Cell pellets were lysed in TRI reagent solution (Ambion) and total RNA was purified. cDNA was synthesized using SuperScript II Reverse Transcriptase (Invitrogen) and transcript levels were quantified on an Applied Biosystems ViiA 7 Real-Time PCR

System instrument using Power Sybr Green PCR Master Mix (Applied Biosystems). PCR primer sequences were the following:

Hk2 (forward 5'-TGTGAAGATGCTGCCACC-3'; reverse 5'-TGTCTGTCCCATCCGGAGT-3') Pkm2 (forward 5'-TT CGCATGCAGCACCTGAT-3'; reverse 5'-CCTCGAATAGC TGCAAGTGGTA-3')

Gli1 (forward 5'-AAGCCAAC TTTATGTCAGGG-3'; reverse 5'-AGAGCCCGCTTCTTTCTTAA-3')

Hprt (forward 5'-GCTTCCTCCTCAGACCGCTT-3'; reverse 5'-GGTCATAACCTGGTTCATCATCG-3')

Results were expressed as fold induction relative to control samples using the $\Delta\Delta C_t$ method with Hprt as an internal control.

Western blotting

GCPs and MB neurospheres were lysed in lysis buffer containing 50 mM Tris-HCl, 2% SDS, 10% Glycerol, 10 mM $\text{Na}_4\text{P}_2\text{O}_7$, 100 mM NaF, 6 M urea, 10 mM EDTA and sonicated. Protein concentration was determined by NanoDrop 1000 spectrophotometer V3.7. 80 μg of proteins were separated by SDS-PAGE, transferred on nitrocellulose membrane and incubated with primary antibodies overnight.

L-lactate measurements

Lactic acid was analyzed as methoxime/tertbutyldimethylsilyl derivatives as previously described.³² Briefly, cells were collected by centrifugation at 1000 rpm for 5 minutes. 20 μL of supernatant were deproteinized by adding 100 μL of acetonitrile and vortexed for 3 minutes. The mixtures were diluted 1:10 with distilled water and centrifuged at 15000 rpm for 15 minutes at 4°C to pellet proteins. The deproteinized supernatant was used to quantify extracellular L-lactate by GC-SIM-MS analysis. Aliquots of 0,25 ml of the supernatant layer spiked with the internal standard (IS) 3,4-dimethoxybenzoic acid (final concentration 1000 ng ml^{-1}) were added to 0,7 ml of distilled water and adjusted to pH ≥ 13 with 7 M NaOH. Methoxylation was performed by adding to the reaction mix methoxyamine hydrochloride (5 mg) at 60°C for 60 min. The samples were then washed with diethylether (3 ml \times 2) and the aqueous phase was adjusted to pH < 2 with concentrated sulfuric acid. The mixture was saturated with NaCl and extracted with diethyl ether (3 ml) and

ethyl acetate (2 ml). The organic extracts were combined in the presence of triethylamine (10 μL) and dried under reduced pressure. The samples were then suspended in 30 μL of toluene subjected to the second derivatization step by adding 20 ml of MTBSTFA (65°C for 30 min) and analyzed by GC-MS. Results were normalized on cell number and expressed as fold change relative to control samples. Each experiment was performed in triplicate and for at least 3 times. Cerebellum and medulloblastoma samples were homogenized in a ice-bath using an ultra-turrax T8 blender with the addition of 1 mL water:acetonitrile (9:1). The homogenized tissue was centrifuged at 13000 g for 15 min at 4°C. 0,25 ml of the cerebellum and medulloblastoma extract were spiked with internal standard (IS) 3,4-dimethoxybenzoic acid (final concentration 1000 ng ml^{-1}) and subjected to methoxylation/ tertbutyldimethylsilylation as described above. Results were normalized on tissue weight and expressed as fold change relative to control samples.

Immunohistochemistry

Immunohistochemical analysis of allografted tumor sections was performed as described.³¹ The following antibodies and conditions were used:

Ki67 (1:200, Leica Biosystems) was diluted in 1% serum PBS-T. Caspase 3 (1:500, Cell Signaling) was diluted in 5% serum PBS-T. Antibodies were incubated for one hour at room temperature. Nuclei were counterstained with hematoxylin in accordance with standard procedures.

Disclosure of Potential Conflicts of Interest

No potential conflicts of interest were disclosed.

Funding

This work was supported by AIRC (Associazione Italiana Ricerca Cancro) grant # IG10610, AIRC 5XMILLE, MIUR FIRB and PRIN projects, Ministry of Health, EU HEALING grant # 238186, Pasteur Institute-Cenci Bolognetti Foundation and Italian Institute of Technology (IIT), NIH P41 RR011823. LDM and SC were supported by fellowships from the Pasteur Insitute-Cenci Bolognetti Foundation.

References

1. Gilbertson RJ, Ellison DW. The origins of medulloblastoma subtypes. *Ann Rev Pathol* 2008; 3:341-65; PMID:18039127
2. Schuller U, Heine VM, Mao J, Kho AT, Dillon AK, Han YG, Huillard E, Sun T, Ligon AH, Qian Y, et al. Acquisition of granule neuron precursor identity is a critical determinant of progenitor cell competence to form Shh-induced medulloblastoma. *Cancer Cell* 2008; 14:123-34; PMID:18691547
3. Wechsler-Reya RJ, Scott MP. Control of neuronal precursor proliferation in the cerebellum by sonic hedgehog. *Neuron* 1999; 22:103-14; PMID:10027293
4. Archer TC, Weeraratne SD, Pomeroy SL. Hedgehog-Gli1 pathway in medulloblastoma. *J Clin Oncol* 2012; 30:2154-6; PMID:22508821
5. Ryan KE, Chiang C. Hedgehog secretion and signal transduction in vertebrates. *J Biol Chem* 2012; 287:17905-13; PMID:22474285
6. Oliver TG, Graseder LL, Carroll AL, Kaiser C, Gillingham CL, Lin SM, Wickramasinghe R, Scott MP, Wechsler-Reya RJ. Transcriptional profiling of the Sonic hedgehog response: a critical role for N-myc in proliferation of neuronal precursors. *Proc Natl Acad Sci U S A* 2003; 100:7331-6; PMID:12777630
7. Taylor MD, Northcott PA, Korshunov A, Remke M, Cho YJ, Clifford SC, Eberhart CG, Parsons DW, Rutkowski S, Gajjar A, et al. Molecular subgroups of medulloblastoma: the current consensus. *Acta Neuropathol* 2012; 123:465-72; PMID:22134537
8. Amakye D, Jagani Z, Dorsch M. Unraveling the therapeutic potential of the Hedgehog pathway in cancer. *Nat Rev Clin Oncol* 2013; 9:1410-22; PMID:24202394
9. Lauth M, Bergstrom A, Shimokawa T, Toftgard R. Inhibition of GLI-mediated transcription and tumor cell growth by small-molecule antagonists. *Proc Natl Acad Sci U S A* 2007; 104:8455-60; PMID:17494766
10. Kim J, Lee JJ, Kim J, Gardner D, Beachy PA. Arsenic antagonizes the Hedgehog pathway by preventing ciliary accumulation and reducing stability of the Gli2 transcriptional effector. *Proc Natl Acad Sci U S A* 2010; 107:13432-7; PMID:20624968
11. Gershon TR, Crowther AJ, Tikunov A, Garcia I, Annis R, Yuan H, Miller CR, Macdonald J, Olson J, Deshmukh M. Hexokinase-2-mediated aerobic glycolysis is integral to cerebellar neurogenesis and pathogenesis of medulloblastoma. *Cancer Metab* 2013; 1(1):1; PMID:24280107; <http://dx.doi.org/10.1186/2049-3002-1-1>

12. Tech K, Deshmukh M, Gershon TR. Adaptations of energy metabolism during cerebellar neurogenesis are co-opted in medulloblastoma. *Cancer Lett* 2014; PMID:24569090
13. Jang M, Kim SS, Lee J. Cancer cell metabolism: implications for therapeutic targets. *Exp Mole Med* 2013; 45:e45; PMID:24091747
14. Marroquin LD, Hynes J, Dykens JA, Jamieson JD, Will Y. Circumventing the Crabtree effect: replacing media glucose with galactose increases susceptibility of HepG2 cells to mitochondrial toxicants. *Toxicol Sci : an official J Soc Toxicol* 2007; 97:539-47; PMID: 17361016
15. Masui K, Tanaka K, Akhavan D, Babic I, Gini B, Matsutani T, Iwanami A, Liu F, Villa GR, Gu Y, et al. mTOR complex 2 controls glycolytic metabolism in glioblastoma through FoxO acetylation and upregulation of c-Myc. *Cell Metab* 2013; 18:726-39; PMID: 24140020
16. Bhatia B, Potts CR, Guldal C, Choi S, Korshunov A, Pfister S, Kenney AM, Nahle ZA. Hedgehog-mediated regulation of PPARgamma controls metabolic patterns in neural precursors and shh-driven medulloblastoma. *Acta Neuropathol* 2012; 123:587-600; PMID:22407012; <http://dx.doi.org/10.1007/s00401-012-0968-6>
17. Beauchamp EM, Ringer L, Bulut G, Sajwan KP, Hall MD, Lee YC, Peaceman D, Ozdemirli M, Rodriguez O, Macdonald TJ, et al. Arsenic trioxide inhibits human cancer cell growth and tumor development in mice by blocking Hedgehog/GLI pathway. *J Clin Invest* 2011; 121:148-60; PMID:21183792; <http://dx.doi.org/10.1172/JCI42874>
18. Teperino R, Amann S, Bayer M, McGee SL, Loipetzberger A, Connor T, Jaeger C, Kammerer B, Winter L, Wiche G, et al. Hedgehog partial agonism drives Warburg-like metabolism in muscle and brown fat. *Cell* 2012; 151:414-26; PMID:23063129; <http://dx.doi.org/10.1016/j.cell.2012.09.021>
19. Bonnet S, Archer SL, Allalunis-Turner J, Haromy A, Beaulieu C, Thompson R, Lee CT, Lopaschuk GD, Puttagunta L, Bonnet S, et al. A mitochondria-K⁺ channel axis is suppressed in cancer and its normalization promotes apoptosis and inhibits cancer growth. *Cancer Cell* 2007; 11:37-51; PMID:17222789; <http://dx.doi.org/10.1016/j.ccr.2006.10.020>
20. Yang ZJ, Ellis T, Markant SL, Read TA, Kessler JD, Bourboulas M, Schuller U, Machold R, Fishell G, Rowitch DH, et al. Medulloblastoma can be initiated by deletion of Patched in lineage-restricted progenitors or stem cells. *Cancer Cell* 2008; 14:135-45; PMID:18691548; <http://dx.doi.org/10.1016/j.ccr.2008.07.003>
21. Vander Heiden MG, Cantley LC, Thompson CB. Understanding the Warburg effect: the metabolic requirements of cell proliferation. *Science* 2009; 324:1029-33; PMID:19460998; <http://dx.doi.org/10.1126/science.1160809>
22. Cao W, Yacoub S, Shiverick KT, Namiki K, Sakai Y, Porvasnik S, Urbanek C, Rosser CJ. Dichloroacetate (DCA) sensitizes both wild-type and over expressing Bcl-2 prostate cancer cells in vitro to radiation. *The Prostate* 2008; 68:1223-31; PMID:18465755; <http://dx.doi.org/10.1002/pros.20788>
23. Madhok BM, Yeluri S, Perry SL, Hughes TA, Jayne DG. Dichloroacetate induces apoptosis and cell-cycle arrest in colorectal cancer cells. *Br J Cancer* 2010; 102:1746-52; PMID:20485289; <http://dx.doi.org/10.1038/sj.bjc.6605701>
24. Sun RC, Fadia M, Dahlstrom JE, Parish CR, Board PG, Blackburn AC. Reversal of the glycolytic phenotype by dichloroacetate inhibits metastatic breast cancer cell growth in vitro and in vivo. *Breast Cancer Res Treat* 2010; 120:253-60; PMID:19543830; <http://dx.doi.org/10.1007/s10549-009-0435-9>
25. Kumar A, Kant S, Singh SM. Novel molecular mechanisms of antitumor action of dichloroacetate against T cell lymphoma: Implication of altered glucose metabolism, pH homeostasis and cell survival regulation. *Chemico-Biolo Interact* 2012; 199:29-37; PMID:22705712; <http://dx.doi.org/10.1016/j.cbi.2012.06.005>
26. Sun W, Zhou S, Chang SS, McFate T, Verma A, Califano JA. Mitochondrial mutations contribute to HIF1alpha accumulation via increased reactive oxygen species and up-regulated pyruvate dehydrogenase kinase 2 in head and neck squamous cell carcinoma. *Clin Cancer Res: an official J Am Assoc Cancer Res* 2009; 15:476-84; PMID:19147752; <http://dx.doi.org/10.1158/1078-0432.CCR-08-0930>
27. Michelakis ED, Sutendra G, Dromparis P, Webster L, Haromy A, Niven E, Maguire C, Gammer TL, Mackey JR, Fulton D, et al. Metabolic modulation of glioblastoma with dichloroacetate. *Sci Translational Med* 2010; 2:31ra4; <http://dx.doi.org/10.1126/scitranslmed.3000677>
28. Canettieri G, Di Marcotullio L, Greco A, Coni S, Antonucci L, Infante P, Pietrosanti L, De Smaele E, Ferretti E, Miele E, et al. Histone deacetylase and Cullin3-REN(KCTD11) ubiquitin ligase interplay regulates Hedgehog signalling through Gli acetylation. *Nat Cell Biol* 2010; 12:132-42; PMID:20081843; <http://dx.doi.org/10.1038/ncb2013>
29. Shi W, Nacev BA, Aftab BT, Head S, Rudin CM, Liu JO. Itraconazole side chain analogues: structure-activity relationship studies for inhibition of endothelial cell proliferation, vascular endothelial growth factor receptor 2 (VEGFR2) glycosylation, and hedgehog signaling. *J Med Chem* 2011; 54:7363-74; PMID:21936514; <http://dx.doi.org/10.1021/jm200944b>
30. Canettieri G, Coni S, Della Guardia M, Nocerino V, Antonucci L, Di Magno L, Screaton R, Screpanti I, Giannini G, Gulino A. The coactivator CRTC1 promotes cell proliferation and transformation via AP-1. *Proc Natl Acad Sci U S A* 2009; 106:1445-50; PMID:19164581; <http://dx.doi.org/10.1073/pnas.0808749106>
31. Coni S, Antonucci L, D'Amico D, Di Magno L, Infante P, De Smaele E, Giannini G, Di Marcotullio L, Screpanti I, Gulino A, et al. Gli2 acetylation at lysine 757 regulates hedgehog-dependent transcriptional output by preventing its promoter occupancy. *PLoS One* 2013; 8:e65718; PMID:23762415; <http://dx.doi.org/10.1371/journal.pone.0065718>
32. Paik MJ, Cho EY, Kim H, Kim KR, Choi S, Ahn YH, Lee G. Simultaneous clinical monitoring of lactic acid, pyruvic acid and ketone bodies in plasma as methoxime/ter-butylidimethylsilyl derivatives by gas chromatography-mass spectrometry in selected ion monitoring mode. *Biomed Chromatogr: BMC* 2008; 22:450-3; PMID:18254151; <http://dx.doi.org/10.1002/bmc.966>